논문 2007-44SC-2-5

# 위상조절 왜곡발생기를 가진 아날로그 전치왜곡기를 이용한 Doherty Amplifier의 선형성 개선

## ( Linearity Improvement of Doherty Amplifier Using Analog Predistorter with Phase-Controlled Error Generator )

이 용 섭*, 정 윤 하*

( Yong-Sub Lee and Yoon-Ha Jeong )

요 약

본 논문은 Doherty 증폭기의 높은 효율을 유지하면서 선형성을 개선하기 위해 아날로그 전치왜곡기를 가진 Doherty 증폭기를 보여준다. 3차 전치왜곡기는 전치왜곡기와 Doherty 증폭기에서 3차와 5차 혼변조 성분이 이루는 위상차를 같게 만들어 3차뿐만 아니라 5차 혼변조 왜곡신호를 동시에 상쇄시킨다. 이것은 전치왜곡기에서 위상조절 왜곡발생기를 이용하여 3차와 5차의 위상차를 독립적으로 조절함으로서 이루어진다. 또한, 간단하고 정확한 위상 측정 장치를 이용하여 왜곡발생기의 위상조절 능력을 실험적으로 확인한다. 실험적인 검증을 위해, 3차 전치왜곡기는 2.11-2.17 GHz의 WCDMA 대역에서 180-W Doherty 증폭기와 구현된다. 투톤 실험결과는 3차와 5차 혼변조 왜곡성분이 크게 상쇄될 수 있음을 보여준다. 또한, 4-carrier WCDMA 응용에서도 넓은 출력 범위에서 상당한 ACLR이 개선된다. 이 기법은 간단한 구조, 작은 크기, 세 가지의 조절 파라미터 때문에 가격 효율적이며 편리하다.

Abstract

This paper represents a Doherty amplifier (DPA) with analog predistorter (PD) to improve the linearity of the DPA while preserving the high efficiency. A third-order PD cancels fifth-order intermodulation (IM5) as well as third-order intermodulation (IM3) components by their same phase difference in the PD and DPA. This is accomplished by independently controlling their phase by using the phase-controlled error generator in the PD. Also, we confirm the phase-control ability of the error generator experimentally with a simple and accurate phase measurement setup. For experimental verification, a third-order PD has been implemented and tested in a 180-W DPA at the wide-band code division multiple access (WCDMA) band of 2.11-2.17 GHz. Two-tone test results show that significant cancellation of IM3 and IM5 components can be obtained. For four-carrier WCDMA applications, significant adjacent channel leakage ratio (ACLR) improvement is achieved over a wide range of output power levels. This technique is cost-effective and convenient due to its simple structure, compact size, and three control parameters.

**Keywords**: Adjacent channel leakage ratio, Doherty amplifier, error generator, phase, predistorter.

## Ⅰ. Introduction

The Doherty amplifier (DPA) can achieve high efficiency at the expense of linearity at high output power and linearization techniques make the Doherty amplifier improve the linearity while preserving efficiency enhancement[1]-[3]. Among linearization techniques for linearity improvement of power amplifiers (PAs), predistortion methods have been adopted frequently in repeaters and base stations. Digital predistortion (DPD) approaches provide high linearity, compactness, and high power efficiency, but are complicated and typically implemented at the

* 정회원, 포항공과대학교
(Pohang University of Science and Technology)
※ This work was partially supported by the BK21 program and the National Center for Nanomaterials Technology (NCNT), Korea.
접수일자: 2006년10월31일, 수정완료일: 2007년2월16일

baseband level[4]-[6]. Analog predistortion techniques, however, work at the radio frequency (RF) with the advantage of simple circuitry, low cost, and moderate linearity improvement[7]-[10].

For conventional analog predistorters (PDs), higher-order intermodulation components become more important due to the limits of linearity improvement in wide-band code division multiple access (WCDMA) applications by only the third-order intermodulation (IM3) cancellation. Fifth-order or more extended PDs enhance linearity to some degree, but are not effective due to their large sizes, complicated structures, and control parameters[11]-[13]. In order to achieve good linearity with the conventional third-order PDs for WCDMA applications, the fifth-order intermodulation (IM5) as well as IM3 components should be cancelled. This can be realized by the same phase difference between the two components in the PD and PA. In [10], Lee et al. report a method that uses the gate bias of a PA to achieve the same phase difference. By controlling the gate bias voltage, the phase difference between IM3 and IM5 components changes and then becomes identical in the PD and PA, whereas the phases change equally by the phase shifter in the PD. Unfortunately, such a technique cannot be employed universally since this result was achieved under special conditions with a combination of the PD, driver, and PA. Therefore, controlling the phase difference between the two components in the third-order PD is the preferred method.

In this paper, we propose a phase-controlled error generator in the PD to cancel the IM3 and IM5 components using the third-order PD. As this error generator controls phases in the PD independently, the IM3 and IM5 components are cancelled simultaneously by their identical phase difference in the PD and DPA. For experimental verification, a 180-W DPA and simple third-order PD are implemented at 2.14 GHz and tested using two-tone and WCDMA signals. The measured results show that IM3 and IM5 components are cancelled, and significant adjacent channel leakage ratio (ACLR) improvement is obtained over a wide range of output power level while preserving high efficiency of the DPA.

## II. Third-Order PD with Phase-Controlled Error Generator

### 1. Operation of proposed third-order PD

If the IM3 and IM5 components are sufficiently generated from the error generator and their magnitude and phase difference is identical in the PD and PA, they can be cancelled simultaneously at the output. Fig. 1 shows the schematic diagram of the proposed third-order PD with the phase-controlled error generator. For a two-tone test, the PA has the IM3 and IM5 components with the specific magnitude and phase difference. Therefore, the IM3 and IM5 components in the PD should have the adequate magnitude and phase difference to cancel the IM3 and IM5 components of the PA. The desired magnitude difference is simply obtained by choosing the appropriate value of a fixed attenuator in front of the error generator. The phase difference is controlled by a series variable capacitor of the phase-controlled error generator. The operation of this error generator is represented below.

If we assume that the reactance at the error generation path only exists, the phase variation is the function of the frequency and capacitance, as shown in [14]. Also, the current $i(t)$ is given by the following equation using the voltage $v(t)$, which is

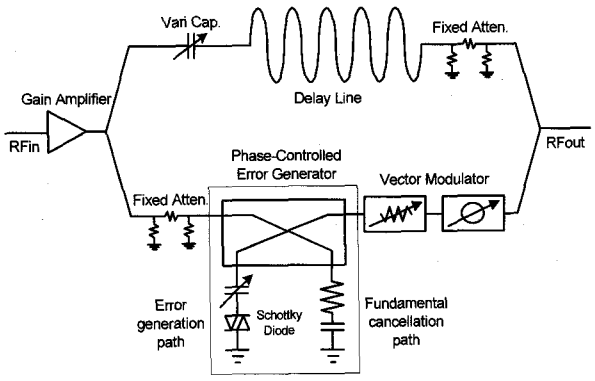


그림 1. 위상조절 왜곡발생기를 가진 제안된 3차 전치 왜곡기의 회로도

Fig. 1. Schematic diagram of the proposed third-order PD with phase-controlled error generator.

applied to an anti-parallel diode configuration.

$$i(t) = I_o[\exp(a_d v(t)) - \exp(-a_d v(t))] \quad (1)$$

where $I_o$ and $a_d$ are constant. The Taylor-series expansion of above equation can be written as

$$i(t) = \sum_{n=1}^{\infty} \alpha_{2n-1} (a_d v(t))^{2n-1} \quad (2)$$

where $\alpha_{2n-1}$ is constant. If a two-tone input signal with the same amplitude and phase given by

$$v(t) = Ae^{j\theta(\omega,c)}[\cos(\omega_1 t) + \cos(\omega_2 t)] \quad (3)$$

is applied to the anti-parallel diode configuration, the IM3 and IM5 components from a pair of diodes can then be expressed as

$$IM3 = \sum_{n=1}^{\infty} C_{3,2n+1} \left(\alpha_{2n+1} a_d A e^{j\theta(\omega,c)}\right)^{2n+1} \quad (4)$$

$$IM5 = \sum_{n=1}^{\infty} C_{5,2n+3} \left(\alpha_{2n+3} a_d A e^{j\theta(\omega,c)}\right)^{2n+3} \quad (5)$$

where $A$ and $\theta$ are the magnitude and phase of the input signal, and $C_{3,2n+1}$ and $C_{5,2n+3}$ are constants.

According to (4), the IM3 components are generated from not only the third-order nonlinear term but also the higher-order terms, and are affected by their magnitudes and phases. The IM5 components suffer from the same mechanism as the IM3 case, as shown in (5). However, phases of the IM3 and IM5 components change independently, since each order nonlinear term serving the IM3 and IM5 generation has different magnitude and phase contributions. This means that the phase difference between the IM3 and IM5 components can be controlled by the phase-controlled error generator.

## 2. The phase measurement of IM components

The phase measurement technique was required to check the phase-control ability of the proposed error generator. The simple and exact method is to use two identical error generators showing the same

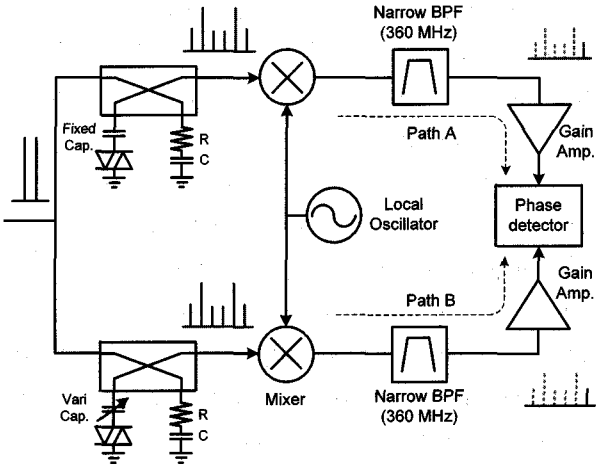


그림 2. 캐패시턴스에 따른 IM 성분의 위상을 측정하기 위한 구성도

Fig. 2. Setup to measure the phases of the IM components according to the capacitance.

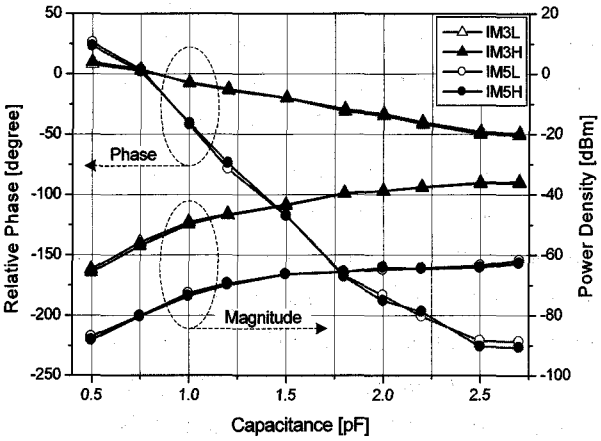


그림 3. 캐패시턴스에 따른 IM3와 IM5 성분들의 측정된 크기와 위상 특성

Fig. 3. Measured phase and magnitude characteristics of the IM3 and IM5 components in the error generator according to the capacitance.

intermodulation distortion (IMD) properties. When the error generator with fixed capacitance is set to the reference, and the capacitance of the other error generator changes, the relative phase change with respect to the capacitance can be accurately measured. Fig. 2 shows the phase measurement setup. Because of the symmetrical structure of this setup, phases of the IM components were varied by only capacitance. The desired IM component was easily selected by the local oscillator (LO) and separated from other signals using the narrow band pass filters (BPFs)[15].

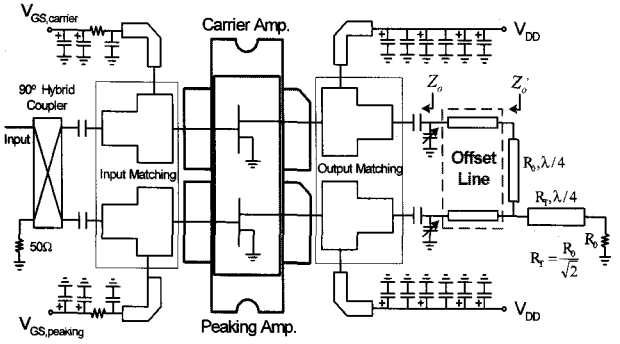


그림 4. 푸쉬풀 형태의 LDMOSFET을 이용한 Doherty 증폭기의 회로도

Fig. 4. Schematic diagram of the DPA using a push-pull type LDMOSFET.

For this measurement, the error generator was implemented using a 3-dB hybrid coupler (Anaren JX503), two Schottky diodes (Agilent HSMS 2850), and an RF35 circuit board ($h$=0.5 mm, $\epsilon_r$=3.5). Capacitance of one error generator (fixed cap.) was fixed at 0.75 pF and the other (vari cap.) ranged from 0.5 pF to 2.7 pF. A resistor (R) of 2.2 Ω and capacitor (C) of 3.9 pF were used to cancel the fundamental signals. The input power level in the error generator was set to -5 dBm.

Fig. 3 shows the measured phase and magnitude characteristics of the IM3 and IM5 components according to the capacitance for two-tone signals with 1-MHz tone spacing at a frequency of 2.14 GHz. From the measured results, the IM5 components initially had phase variation greater than that of the IM3 components, and had dominant influence on the phase difference between the two components, showing the symmetric magnitude and phase characteristics between the lower and upper band. Thus, it is possible to independently control the IM5 phase in the PD, as described in section II-1. Additionally, since the phase difference between the two components was found to be over 180°, the IM3 and IM5 components can be cancelled out at the same time, independent of the phase difference in the PA. We found that the phase-controlled error generator in the PD had the ability to control the phases of the IM5 components and cancel out the IM5 components. Although they suffer from magnitude variations by the capacitance, this problem is overcome by the attenuator in the PD due to the similar magnitude characteristics according to the capacitance. The delay mismatch resulting from the capacitance change in the error generator is compensated by a variable capacitor on the upper path, as shown in Fig. 1.

## III. Implementation and Experimental Results

### 1. Implementation

The DPA has been implemented using a Freescale's push-pull type MRF21180 LDMOSFET (180-W PEP) and RF35 ($h$=0.5 mm, $\epsilon_r$=3.5) circuit board at the WCDMA band of 2.11-2.17 GHz, as shown in Fig. 4. The input and output impedances of the carrier and peaking amplifiers have been matched to R0=50Ω. The matching circuits of each amplifier have been individually optimized to achieve good performance. In the process of determining the optimum length of the offset line, $Z_o$=7+j11.5Ω has been transformed to $Z_o'$=365Ω by the 0.214λ (76.9°) length of 50Ω offset line. To reduce the memory effects, the drain bias circuit incorporates a quarter-wave bias line with a 2-mm line width and several decoupling capacitors -5.1 pF for the RF and 1 nF, 220 nF, 4.7 μF, 10 μF, 15 μF, and 100 μF for the modulation frequency. In the case of the DPA,

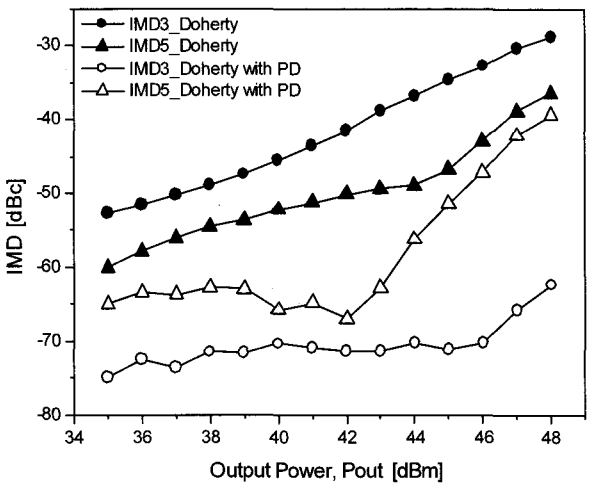


그림 5. 출력전력에 따른 측정된 IMD 특성

Fig. 5. Measured IMD characteristics as a function of output power levels.

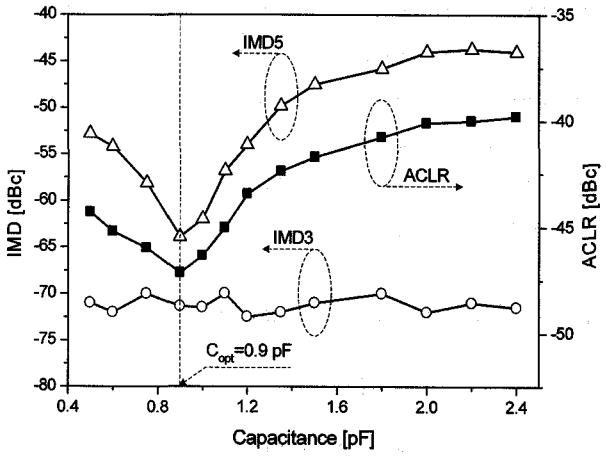


그림 6. 출력전력 42 dBm에서 캐패시턴스에 따른 IMD 특성

Fig. 6. IMD characteristics according to capacitance at a Pout of 42 dBm.

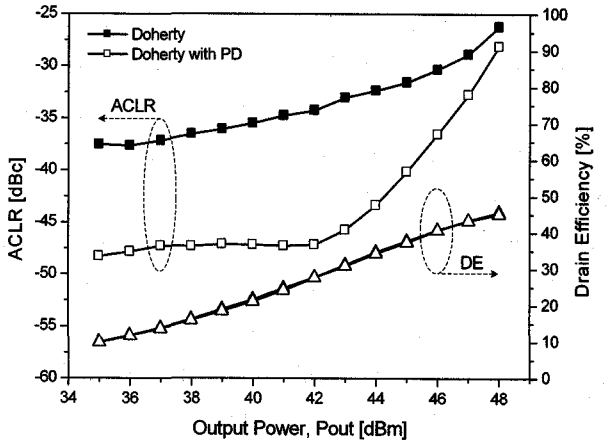


그림 7. 4-carrier WCDMA 신호에 대한 출력전력에 따른 측정된 ACLR과 드레인 효율 특성

Fig. 7. Measured characteristics of ACLR and drain efficiency according to output power for four-carrier WCDMA signals.

the quiescent drain currents of the carrier and peaking amplifier have been biased to class AB ($V_{GS}$=3.783 V) and class C ($V_{GS}$=1.87 V) at a $V_{DD}$ of 28 V, respectively.

In the third-order PD in Fig. 1, the gain amplifier had a gain of 14.2 dB at a VDD of 5 V and the loss of the linear path, which contained two 3-dB couplers and a delay line, was 7.2 dB. Therefore, the $\pi$-type fixed attenuator of 7 dB was inserted between a 3-dB hybrid coupler and the delay line to make the input and output power levels of the PD identical. At the nonlinear path, a 1.5-dB fixed attenuator before the error generator was used to produce the IM3 and IM5 components with the proper magnitude difference. To obtain the sufficient control range of the vector modulator, an attenuator and two phase shifters were used. Also, the murRata's chip trimmer capacitor was used to compensate for the delay mismatch in the upper path.

## 2. Experimental Results

To improve the linearity of the DPA for the WCDMA applications, it is necessary to cancel out the IM5 as well as IM3 components for a two-tone test. Thus, we performed a two-tone test and four-carrier WCDMA signal test at a frequency of 2.14 GHz. All results for WCDMA signals have been measured in symmetrical state between the lower- and upper-band ACLR at ±5 MHz offset from the center frequency of the uppermost and lowermost channel. The measured IMD characteristics as a function of output power levels for a two-tone signal with 1-MHz tone-spacing are shown in Fig. 5. The phase-controlled capacitor of the error generator in the PD has been optimized at a Pout of 42 dBm and the vector modulator in the PD has been controlled optimally at each output power level.

The DPA with the proposed PD not only cancels the IM3 components below -70 dBc at a wide range

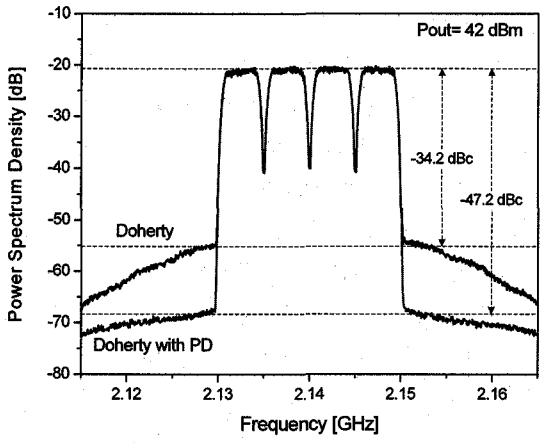


그림 8. 4-carrier WCDMA 신호에 대한 출력전력 42 dBm에서의 Doherty 증폭기의 전력 스펙트럼

Fig. 8. Power Spectrum densities of the proposed DPA at a Pout of 42 dBm for a four-carrier WCDMA signal.

of output power levels but also significantly reduces the IM5 component at a Pout of 42 dBm.

Fig. 6 shows the measured IMD and ACLR variations according to capacitance at a Pout of 42 dBm. The vector modulator in the PD has been optimized at each capacitance. From experimental results, the perfect cancellation of IM3 components is achieved at any capacitance, but the maximum cancellation of the IM5 components occur at a capacitance of 0.9 pF, which is the optimum capacitance ($C_{opt}$). Additionally, ACLR characteristics are improved significantly at this point. Thus, it is experimentally justified that the phase-controlled error generator can control the phase difference between the IM3 and IM5 components in the PD and heavily contribute to the IM5 reduction of the PA. The measured ACLR characteristics of the proposed PD for a four-carrier WCDMA signal are shown in Fig. 7, when the output power level is swept. The good ACLR characteristics are achieved over a whole output power range. For the proposed PD, the maximum ACLR improvement of 13 dB is obtained at a Pout of 42 dB, as shown in Fig. 8.

## Ⅳ. Conclusion

We have proposed a simple and effective predistortion technique to cancel the IM3 and IM5 components of the DPA using the third-order analog PD. The IM3 and IM5 components were cancelled out simultaneously by their identical phase difference in the PD and DPA. This was accomplished by controlling the phase difference with the help of the phase-controlled error generator in the PD. Also, we confirmed the phase-control ability of this error generator using a simple and accurate phase measurement setup. To verify this method, the analog third-order PD was implemented in a 180-W DPA operating at WCDMA band of 2.11-2.17 GHz. We observed significant cancellation in the IM5 as well as IM3 components for a two-tone test. We also achieved superior ACLR performance for four-carrier WCDMA signals over a wide operating power range. Owing to its simplicity in structure and control parameters, this technique can easily be applied to linear PAs, and potentially combined with adaptive control circuits.

## References

[1] S. C. Cripps, Advanced Techniques in RF Power Amplifiers Design, Norwood, MA: Artech House, 2002.

[2] Y. G. Yang, J. H. Cha, B. J. Shin, and B. M. Kim, "A Fully Matched N-Way Doherty Amplifier with Optimized Linearity," IEEE Trans. Microw. Theo- ry Tech., vol. 51, no. 3, pp. 986-993, Mar. 2003.

[3] Y. S. Lee, S. Y. Lee, K. I. Jeon, and Y. H. Jeong, "Linearity Improvement of Doherty Amplifier Using Analog Predistorter for WCDMA Applications," in Pro. of 36th European Microw. Conf., Manchester, UK, pp. 1205-1208, Sep. 2006.

[4] S. P. Stapleton, "Amplifier linearization using adaptive digital predictortion," Appl. Microw. Wireless, vol. 13, pp. 72-77, Feb. 2001.

[5] S. Boumaiza and F. M. Gahnnouchi, "Realistic power-amplifiers characterization with application to base baseband digital predistortion for 3G base stations," IEEE Trans. Microw. Theory Tech., vol. 50, no. 12, pp. 3016-3021, Dec. 2002.

[6] N. Ceylan, J. E. Mueller, and R. Weigel, "Optimization of EDGE terminal power amplifiers using memoryless digital predisto- rtion," IEEE Trans. Microw. Theory Tech., vol. 53, no. 2, pp. 515-522, Feb. 2005.

[7] B. Albeiner, "The concept of predistortion," Microw. J., vol. 46, no. 10, pp. 82-102, Oct. 2003.

[8] J. Cha, J. Yi, J. Kim, and B. Kim, "Optimum design of a predistortion RF power amplifier for multi-carrier WCDMA applications," IEEE Trans. Microw. Theory Tech., vol. 52, no. 2, pp. 655-663, Feb. 2004.

[9] S. Y. Lee, Y. S. Lee, S. H. Hong, H. S. Choi, and Y. H. Jeong, "An Adaptive Predistortion RF Power Amplifier With a Spectrum Monitor for Multicarrier WCDMA Applications," IEEE Trans. Microw. Theory Tech., vol. 53, no. 2, pp. 786-793, Feb. 2005.

[10] S. Y. Lee, Y. S. Lee and Y. H. Jeong, "Fully-automated adaptive analog predistortion power amplifier in WCDMA applications," in Proc. of 35th European Microw. Conf., Paris, France, pp. 967-970, Oct. 2005.

[11] J. Yi, Y. Yang, M. Park, W. Kang, and B. Kim, "Analog predistortion linearizer for high-power RF amplifiers," IEEE Trans. Microw. Theory Tech., vol. 48, no. 12, pp. 2709-2713, Dec. 2000.
[12] Y. Yang, Y. Y. Woo, and B. Kim, "New predistortion linearizer using low-frequency even-order intermodulation components," IEEE Trans. Microw. Theory Tech., vol. 50, no. 2, pp. 446-452, Feb. 2002.
[13] S. Y. Lee, Y. S. Lee, S. H. Hong, H. S. Choi, and Y. H. Jeong, "Independently controllable 3rd- and 5th-order analog predistortion linearizer for RF power amplifier in GSM," in Proc. of IEEE Asia-Pacific Conf. on Advanced System Integrated Circuits, pp. 146-149, Fu- kuoka, Japan, Aug. 2004.
[14] P. Kenington, Hgih-lnearity RF Power Amplifier Design. Norwood, MA: Artech House, 2000, pp. 368-371.
[15] S. Y. Lee, Y. S. Lee, and Y. H. Jeong, "A novel phase measurement technique for IM3 components in RF power amplifiers," IEEE Trans. Microw. Theory Tech., vol. 54, no. 1, pp. 451 -457, Jan. 2006.

## 저 자 소 개

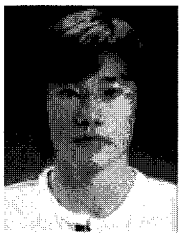

이 용 섭(정회원)
2003년 2월 광운대학교 전자공학과(공학사),
2005년 2월 포항공과대학교 전자전기공학과(공학석사),
2005년 3월~현재 포항공과대학교 전자전기공학과 박사과정.
<주관심분야 : High efficiency RF Power Amplifier design and Linearization Techniques>

정 윤 하(정회원)
1974년 2월 경북대학교 전자공학과 (공학사),
1976년 2월 경북대학교 전자공학과 (공학석사),
1987년 3월 동경대학교 전자공학과 (공학박사),
1987년 2월~1992년 3월 포항공과대학교 전자전기공학과 조교수,
1992년 3월~1997년 3월 포항공과대학교 전자전기공학과 부교수,
1997년 4월~현재 포항공과대학교 전자전기공학과 정교수,
2001년~현재 나노기술연구센터 소장,
2004년~현재 국가 나노기술집적센터 소장 사업단장.
<주관심분야 : RF circuit design, microwave and millimeter-wave device fabrication, single electron transistors, nano-CMOS devices, OTFT>